EDDY CURRENT THERMOGRAPHY NDT OF MULTILAYER HTS TAPES

W. Dirahoui, H. Menana, M. Hinaje

Université de Lorraine, GREEN, F-54000, Nancy, France.
hocine.menana@univ-lorraine.fr

Keywords: Multilayer HTS tapes, control, eddy current thermography, modeling, measurements.

Abstract

Numerical and experimental studies on structural control of multi-layered high-temperature superconductor tapes at room-temperature using eddy-current thermography are presented. A rotating magnet wheel is used as an inductor. A three-dimensional integro-differential formulation in terms of the electric vector potential is developed for eddy current calculations in the HTS tape, where the integral part is discretized by a collocation method, and the differential part is discretized by the finite difference method, coupled with a thermal modeling using the diffusion equation, discretized by the finite difference method. The source magnetic field is calculated using the surface magnetic charge model. Simulation results are confirmed by measurements.

1 Introduction

Rare-earth-based multilayer high-temperature superconductor (HTS) tapes are promising conductors for power applications. However, due to the specific manufacturing process and to a multilayer structure, defects such as non-uniformity and delamination may be occur in such tapes [1,2]. Structural defects can significantly degrade HTS tape performance, therefore, non-destructive characterization to investigate non-uniformities and defects is important for quality control of such tapes in the manufacturing process. Several techniques have been successfully used to control the superconducting properties of such tapes [3, 4].

In this work, we present numerical and experimental investigations for controlling structural defects in 2G-HTS tapes at room temperature using eddy current thermography (ECT). An experimental setup has been developed where a rotating magnet wheel inductor is used to avoid thermal disturbances. A fast 3-D magnetothermal modeling approach has been developed for interpretation of results and simulation of experimentally irreproducible situations. The magnetothermal model is based on combining an integro-differential formulation in terms of the electric vector potential for the eddy current evaluation in the HTS tape subjected to a time-varying external magnetic field generated by a rotating magnet wheel, calculated using the surface magnetic charge model, with a thermal model based on the diffusion equation discretized by the finite difference method.

2 The modelled system

The system, modelled in Cartesian coordinates, and shown in Fig. 1, consists of a multilayer HTS tape exposed to an external magnetic field generated by a magnetic wheel rotating in the y-z plane.

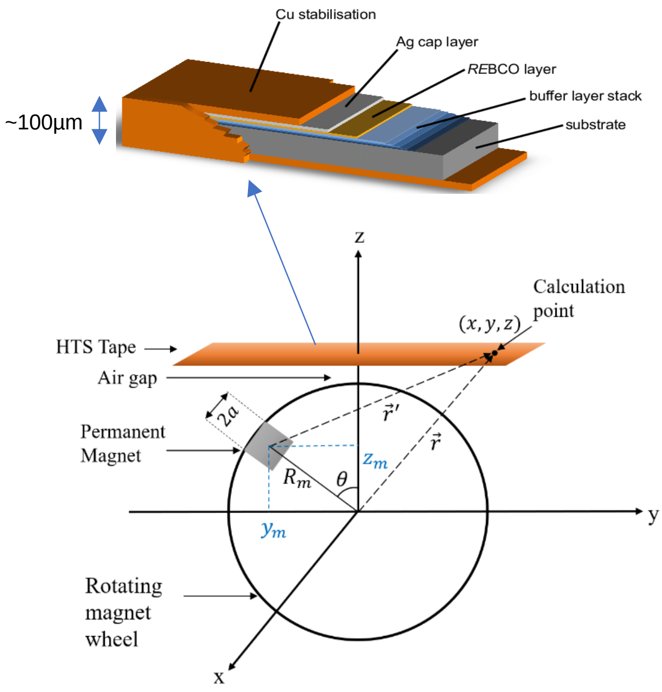

Figure 1: The modelled system.

Due to the thin structure of the HTS tape, the eddy currents are assumed to flow in the $x-y$ plane, and the formulation, given by (1), involves only the normal component of the source magnetic-flux density $\vec{B}_z^s$ and the normal component ($\vec{T}_z$) of the electric vector potential, with $\vec{T}_z = \vec{0}$ on the tape borders.

$$\vec{\nabla} \times \bar{\bar{\sigma}}^{-1}\, \vec{\nabla} \times \vec{T}_z = -\partial_t \left(\vec{B}_z^s + \frac{\mu_0}{4\pi} \int_v \frac{\vec{\nabla} \times \vec{T}_z \times \vec{r}}{r^3} dv \right) \quad (1)$$

In (1), μ_0 and $\bar{\bar{\sigma}}$ are, respectively, the vacuum permeability and the electrical conductivity matrix. The surface magnetic charge model for cuboidal magnets, having a uniform magnetization [6,7], is used to evaluate the source magnetic-flux density generated by the rotating wheel. The z component (normal to the tape surface) of the latter is given by (2).

$$\vec{B}_z^s = \left\{ \frac{B^r}{4\pi} \sum_{i=0}^{1} \sum_{j=0}^{1} \sum_{k=0}^{1} (-1)^{i+j+k} atan2(SW, RU) \right\} \vec{e}_z \qquad (2)$$

where,

$$\begin{cases} S = x - (-1)^i a \\ W = (y + R_m sin\theta) - (-1)^j a \\ U = (z - R_m cos\theta) - (-1)^k a \\ R = \sqrt{S^2 + W^2 + U^2} \end{cases} \qquad (3)$$

In (3), a represents the half length of the cubic magnets edge and R_m is the distance between the wheel and the magnets centres, as illustrated in Figure 1, where (x, y, z) and $(x_m, y_{m,} z_m)$ represent, respectively, the coordinates of the calculation point and that of the center of a magnet. The angular position of the magnetic wheel is related to its rotation speed (Ω), such as $\theta = \Omega t$, where t is the time.

Thermal phenomena caused by joule losses in the tape are governed by the heat diffusion equation given in (4), where, λ, γ, Cp, h, T_e, Γ and $\vec{n}$ are, respectively, the thermal conductivity, the mass density, the specific heat capacity, the convection exchange coefficient, the surrounding medium temperature, the frontier of the tape region and the vector normal to it.

$$\begin{cases} \gamma C_p \dfrac{\partial T}{\partial t} = \dfrac{\partial}{\partial x}\left(\lambda \dfrac{\partial T}{\partial x}\right) + \dfrac{\partial}{\partial y}\left(\lambda \dfrac{\partial T}{\partial y}\right) + \dfrac{\partial}{\partial z}\left(\lambda \dfrac{\partial T}{\partial z}\right) + \mathcal{P} \\ -\lambda \vec{\nabla} \mathrm{T}.\vec{\mathrm{n}} = h(T - T_e), \qquad on\ \Gamma \end{cases} \qquad (4)$$

For the numerical analysis, (4) is discretized using the finite difference method. All the system specifications are given in [8].

Figure 2 shows a comparison between the simulation and the experimental results at steady state. A good match is found between the results. For the experimental results we can notice an asymmetry in the temperature profile along the HTS tape. This asymmetry is due to the aerodynamics of the rotating magnet wheel, creating a cooling imbalance on the tape surface. Indeed, the wheels draw air in one direction and expel it in the other. This was confirmed by reversing the direction of rotation of the magnet wheel. This phenomenon is not considered in the modeling, which only considers a symmetrical increase in the convection coefficient due to the air forced by the rotating wheel.

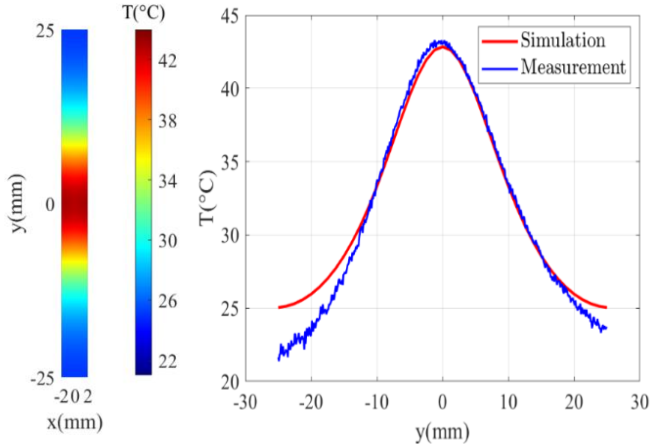

Figure 2: Thermal mapping on the surface of the HTS tape profiles of the temperature along its length at x = 0 mm.

References

[1] T. Matsuda, T. Okamura, M. Hamada et al., “Degradation of the Performance of an Epoxy Impregnated REBCO Solenoid due to Electromagnetic Forces,” Cryogenics, vol. 90, pp. 47–51, (2018).

[2] A. Gorospe et al., "Delamination Characteristics in Wide REBCO Coated Conductor Tapes Under Transverse Loading," IEEE Trans. Appl. Supercond, vol. 25, no. 3, pp. 1-5, Art no. 7200205, (2015).

[3] F S. Wells, A V. Pan, S. Wilson et al., “Dynamic Magneto-Optical Imaging of Superconducting Thin Films,” Supercond. Sci. Technol, vol. 29, no. 3, Art. no 035014 (2016).

[4] K. Higashikawa, D. Uetsuhara, M. Inoue et al., "Characterization of Local Critical Current Distribution in Multifilamentary Coated Conductor Based on Reel-to-Reel Scanning Hall-Probe Microscopy," IEEE Trans. Appl. Supercond, vol. 27, no. 4, pp. 1-4, Art no. 6603004, (2017).

[5] H. Menana and M. Féliachi, "An Integro-Differential Model for 3-D Eddy Current Computation in Carbon Fiber Reinforced Polymer Composites," IEEE Trans. Magn, vol. 47, no. 4, pp. 756-763, (2011).

[6] G. Akoun and J.-P. Yonnet, "3D Analytical Calculation of the Forces Exerted Between Two Cuboidal Magnets," IEEE Trans. Magn., vol. 20, no. 5, pp. 1962-1964, (1984).

[7] J.W. Jansen, J.L.G. Janssen, J.M.M. Rovers, J.J.H. Paulides and E.A. Lomonova, "(Semi-) analytical models for the design of high-precision permanent magnet actuators", International Compumag Society Newsletter, vol. 16, no. 2, pp. 4-17, (2009).

[8] W. Dirahoui, H. Menana, M. Hinaje, "Nondestructive Testing of Multilayer HTS Tapes by Using Eddy Current Thermography", IEEE Trans. on App. Supercond., 32 (8), pp.1-7, (2022).